Structural and Conduction Mechanisms Studies in Strontium Lanthanum Titanate Perovskite SLT Ceramic

H.M.El-Mallah [(1)] *and M.S.Aziz* [(2)]

[(1)] *Department of Physics & Mathematical Engineering, Faculty of Engineering, Suez Canal University, Port-Said, Egypt.*
[(2)] *physics Department, Faculty of Science, Mansoura University, Damietta, Egypt.*

The current – voltage (I–V) characteristics and electric conduction mechanisms for a bulk ceramic perovskite system of the compositions $Sr_{(1-x)}La_xTiO_3$ (SLT) with (x = 0.05, 0.1 and 0.2) have been investigated at different temperatures between (294K-523K). At low voltage region, the conduction was found to be due to thermally generated carriers. At higher voltages, the conduction mechanism was satisfactory explained by the modified Pool–Frenkel type. It was found that the samples possess a typical semiconductor-like behaviour. The activation energy decreased with increasing La content. The effect of composition and temperature on electrical conductivity, the field lowering coefficient $\beta_{exp.}$ and the activation energy E_a have been studied.

1. Introduction:

The perovskite structure (A'A")BO$_3$ has been central to many of the recent development in solid state chemistry, including high – temperature superconductivity and colossal magnetoresistance. Progress in these research areas has relied on the ability of this structure type to accommodate a wide range of chemical substitutions over both the A site (Ideally 12 coordinate) and the B site (Ideally 6 coordinate). The substitution of trivalent cations (La^{+3} or A") onto an A sublattice occupied by divalent cations (Sr^{+2} or A') is usually charge- compensated by the reduction of a transition metal cation on the B site (Ti^{+4}). Alternatively, the introduction of A^{+3} into a compound A^{+2}BO$_3$ can be accommodate by the introduction of vacancies on the A sublattice. Recently, the perovskite-type titanium oxide SLT has been intensively studied as an

example of such systems [1-3]. It is very important in materials science, physics and earth science for their distinguished electrical and optical properties [4 - 8]. It is known that strontium titanate has an ideal cubic structure of the perovskite type [9], and lanthanum titanate crystallizes in an orthorhombically distorted structure of the perovskite type [10]. Latter complex compound $(A'A'')BO_3$ as $LaTiO_3$ is a typical Mott-Hubbard insulator with the d^1 configuration, whereas $SrTiO_3$ is the band insulator with the d^0 configuration. Therefore, one can control the band filling by substituting La^{+3} with Sr^{+2}. Little few data are available on the electrical properties of such compositions.

The present work deals with the studies of the electrical conduction mechanism dependence on the voltage and temperature for SLT system of perovskite structure.

2. Experimental:

2.1. Sample preparation and characterization.

SLT ceramics of chemical composition $Sr_{(1-x)}La_xTiO_3$ (x = 0.05, 0.1 and 0.2) were prepared by using the mechanical techniques [11]. $LaTiO_3$ and $SrTiO_3$ powders (purity > 99.9%) were weighted in the appropriate proportions. The powders were thoroughly mixed together in acetone using a pascall ceramic Ball mill. The mixed powders were dried and then fired at 1573 K for 24 hours, then cooling to room temperature with a rate of 1.67 $^{\circ}C$ min^{-1}, reground and pressed under 1.08 x 10^9 Pa into small discs of diameter 1.3 cm and different thickness using a hydraulic press. These discs were then put in alumina crucible provided with a lid and fired at temperature of 1623 K for 24 hours. They were cooled, crushed, ground, repressed and fired in the same conditions.

The room temperature study of the structure of SLT system was accomplished using X-ray powder diffraction (XRD) in a Philips diffractometer with Cuk_α-radiation with λ=1.5418Å. Data were recorded for 2θ between 10º and 90º in steps of 0.02º. Lattice Parameters of the specimens were determined from X-ray diffraction patterns by the least square method [12].

2.2. D.C. electrical conductivity measurements.

The D.C. electrical measurements on the samples were carried out using a holder with two electrodes. Silver paste was applied to opposite sides of the ceramic plates of diameters 1.3 cm and thickness in the range 0.16 – 0.22 cm, which were then placed in a small furnace. The temperature was measured to better than 1°C with calibrated Ni/NiCr thermocouple which was set close to one of the electrodes. The current voltage, I-V, measurements were carried out using a regulated power supply connected in series with the sample under

investigation and a standard resistor (4.7×10^6 ohm). The current through the samples was calculated by accurately measuring the potential drop across the standard resistor using a digital millimeter (M890G), while the voltage across the samples was obtained as a difference between supply voltage and drop across the standard resistor.

3. Results and Discussion:

3.1. Structural properties.

The XRD patterns of $Sr_{0.95}La_{0.05}TiO_3$, $Sr_{0.9}La_{0.1}TiO_3$ and $Sr_{0.8}La_{0.2}TiO_3$ are shown in Fig. (1). The diffractograms showed no traces other than the intended compositions. All samples crystallized in a perovskite cubic crystal structure. The calculated d-spacing for the samples in comparison with ICDD No. 84-0444 for $SrTiO_3$ and 79-0178 for $Sr_{0.9}La_{0.1}TiO_3$ are reported in Table(1). The calculated lattice parameters for the samples with x = 0.05, 0.1 and 0.2 are a = 3.9016 Å, 3.8961 Å and 3.8848 Å, respectively, which agree with the other studies [13-15]. As observed, the values of the lattice parameters decrease with an increase in La content. The same results have also been found of such system [16-18]. These results may be interpreted by the fact that doped La ions occupy Sr ion sites and has smaller ionic radius (La = 1.04 Å) than the Sr ion (Sr = 1.18 Å) [19].
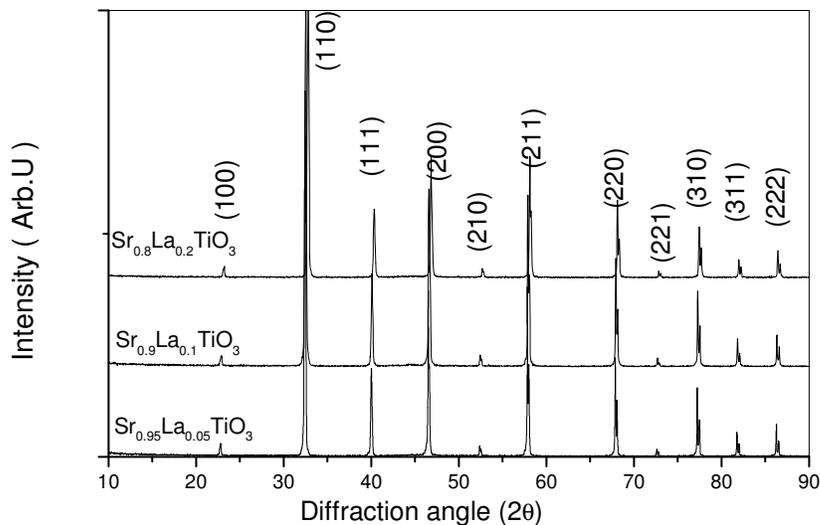
Fig. (1) X-ray diffractogram of SLT ceramic.

Table (1): d - spacing for $Sr_{(1-x)}La_xTiO_3$ ceramics and in comparison with ICDD cards.

No	Sample 1 (x = 0.05)		Sample 2 (x = 0.1)		Sample 3 (x = 0.2)		SrTiO₃ ICDD No. (84-0444)		Sr₀.₉La₀.₁TiO₃ ICDD No. (79-0178)		hkl
	d(Å)	I/I₀	d(Å)	I/I₀	d(Å)	I/I₀	d (Å)	I/I₀	d(Å)	I/I₀	
1	3.8954	3.57	3.8809	2.37	3.8236	3.89	3.9050	3.6	3.9061	4.8	100
2	2.7570	100	2.7497	100	2.7265	100	2.7612	100	2.7620	100	110
3	2.2521	24.3	2.2482	22.0	2.2352	23.6	2.2545	19	2.2551	18.2	111
4	1.9509	45.9	1.9483	41.6	1.9389	40.3	1.9525	35.8	1.9530	35.1	200
5	1.7451	2.67	1.7433	2.67	1.7365	3.17	1.7463	2	1.7468	2.6	210
6	1.5931	48.1	1.5916	41.2	1.5864	45.4	1.5942	28.5	1.5946	31.3	211
7	1.3798	29.2	1.3787	26.6	1.3755	28.7	1.3806	15.6	1.3810	16.3	220
8	1.3010	2.01	1.2999	2.10	1.2975	2.32	1.3016	1	1.3020	1.3	221
9	1.2343	20.4	1.2335	18.6	1.2314	18.9	1.2348	9.5	1.2352	11.6	310
10	1.1770	7.18	1.1761	6.84	1.1744	6.61	1.1774	3.4	1.1777	3.4	311
11	1.1268	9.59	1.1262	7.84	1.1249	9.94	1.1272	4.1	1.1275	4.6	222

3.2. Conduction mechanisms studies.

Figure (2a-c) shows a typical set of results of the current–voltage (I-V) characteristics of the investigated SLT system at different temperatures between (293 – 523 K). It is observed that the current increases with the gradual increase of the applied voltage. The I–V characteristics follow the relation [20]:

$$J = J_o \exp (e \, \beta_{exp.} \, E^{1/2} / k_B T) \qquad (1)$$

where J_o is the pre-exponential factor, k_B is Boltzmann's constant, T the absolute temperature and $\beta_{exp.}$ is the field lowering coefficient, it is an essential factor that determines the magnitude of the Coulombic field [21]. The non linear change in the I–V characteristics can be attributed to either the changes in quasi-equilibrium within the material which may be due to the applied voltage [22]. According to Equation (1) and the data in Fig. 3(a, b and c), which shows the plots of ln J versus $E^{1/2}$, the coefficient β_{exp} can be calculated from the slope of lnJ versus $E^{1/2}$ relations as presented in Table (2) for all samples and temperatures.
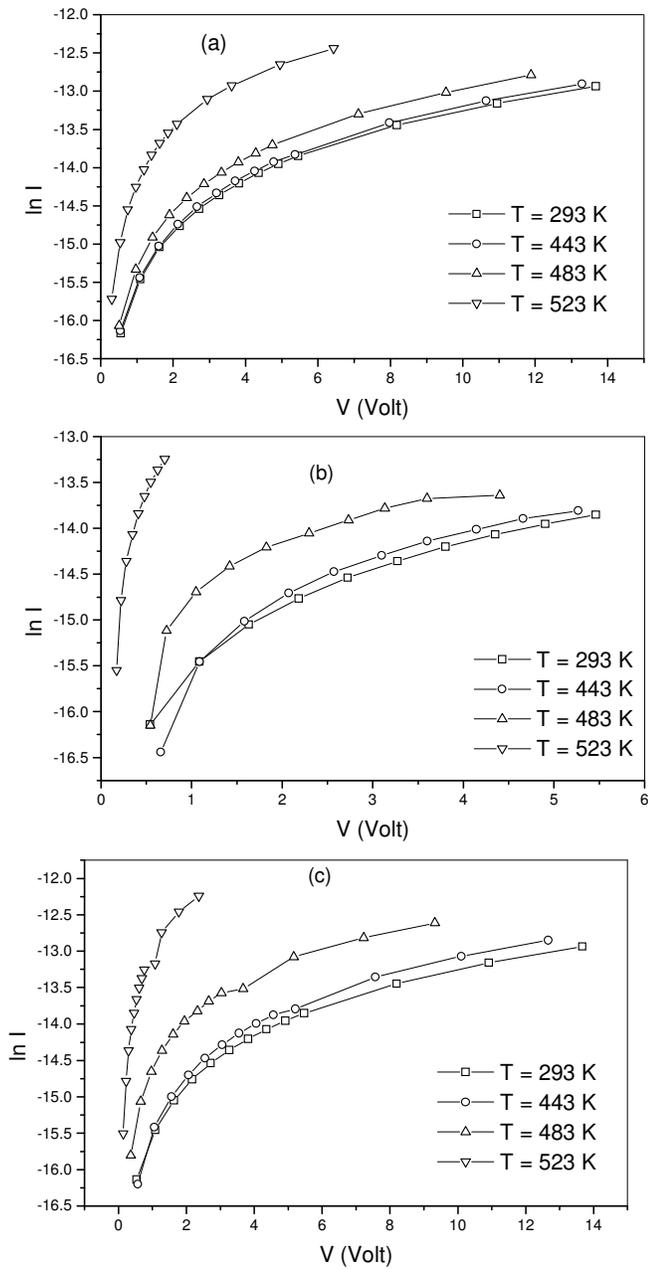
Fig. (2). Current-Voltage characteristics at different temperatures
for SLT ceramics. a) $Sr_{0.95}La_{0.05}TiO_3$. b) $Sr_{0.9}La_{0.1}TiO_3$.
and c) $Sr_{0.8}La_{0.2}TiO_3$.
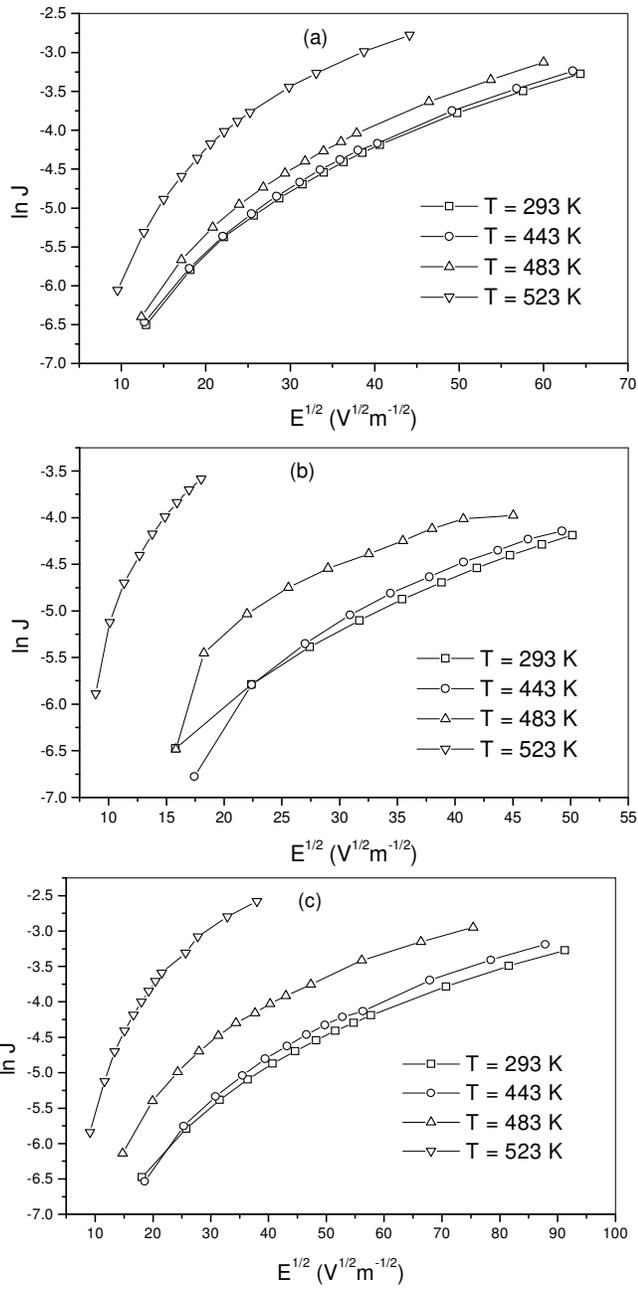
**Fig. (3) Plot of lnJ versus E$^{1/2}$ at different temperatures for
a) Sr$_{0.95}$La$_{0.05}$TiO$_3$. b) Sr$_{0.9}$La$_{0.1}$TiO$_3$. and c)** Sr$_{0.8}$La$_{0.2}$TiO$_3$.

Table (2): Variation of the experimental values of $\beta_{exp.}$ (Poole-Frenkel Model) with compositions and temperatures for SLT ceramics.

Tep (K)	$Sr_{0.95}La_{0.05}TiO_3$		$Sr_{0.9}La_{0.1}TiO_3$		$Sr_{0.8}La_{0.2}TiO_3$	
	$LnJ \& E^{1/2}$	$lnJE^{-1} \& E^{1/2}$	$LnJ \& E^{1/2}$	$lnJE^{-1} \& E^{1/2}$	$LnJ \& E^{1/2}$	$lnJE^{-1} \& E^{1/2}$
	$\beta_{exp}/10^{-3}$ $eVm^{1/2}V^{-1/2}$	β_{exp} $eVm^{1/2}V^{-1/2}$	$\beta_{exp}/10^{-3}$ $eVm^{1/2}V^{-1/2}$	β_{exp} $eVm^{1/2}V^{-1/2}$	$\beta_{exp}/10^{-3}$ $eVm^{1/2}V^{-1/2}$	β_{exp} $eVm^{1/2}V^{-1/2}$
293	0.9685	1.99×10^{-5}	1.066	3.307×10^{-5}	0.6920	1.970×10^{-5}
443	1.529	3.248×10^{-5}	1.508	1.935×10^{-4}	1.140	6.374×10^{-5}
483	1.714	1.832×10^{-5}	1.160	9.106×10^{-4}	1.180	2.376×10^{-4}
523	2.108	3.529×10^{-4}	1.031	3.333×10^{-3}	2.575	5.309×10^{-4}

For comparison, the calculated values applying the following equation:

$$2 \, \beta_{PF} = \beta_{SC} = (e / 4\pi \, \epsilon_o \, \epsilon_r)^{1/2} \qquad\qquad (2)$$

where β_{PF} and β_{SC} are the Poole-Frenkle and Schottky field lowering coefficients, respectively, e the electronic charge, ϵ_o is the space permittivity and ϵ_r the relative permittivity. By taking the high frequency of the relative permittivity ϵ_r obtained from the refractive index n at room temperature ($\epsilon_r = n^2$) as was determined optically by the authors as $n_1 = 2.05$, $n_2 = 1.36$ and $n_3 = 1.31$ for the three tested compositions, respectively, β_{PF} and β_{SC} are calculated from Eq. (2). The calculated values of β_{PF} and β_{SC} for all samples are reported in Table (3). From this Table, we can notice that, the experimental values of $\beta_{exp.}$ do not agree neither with the calculated values of β_{SC} nor that of β_{PF}; this may be due to the low electric field which is used or the nature of the sample itself or all these factors together.

Table (3): Variation of ϵ_r, E_a, β_{PF} and β_{SC} with composition of SLT ceramics.

Composition	Dielectric constant ϵ_r	$\beta_{PF}/10^{-5}$ $(eVm^{1/2}V^{-1/2})$	$\beta_{SC}/10^{-5}$ $eVm^{1/2}V^{-1/2}$	E_a (eV) at 10V
$Sr_{0.95}La_{0.05}TiO_3$	4.188	3.706	1.853	0.185 (±0.010)
$Sr_{0.9}La_{0.1}TiO_3$	1.843	5.586	2.793	0.180 (±0.005)
$Sr_{0.8}La_{0.2}TiO_3$	1.716	5.789	2.895	0.146 (±0.004)

Using the modification of Poole–Frenkle mechanism, from the measured slope of linear part of ln JE^{-1} versus $E^{1/2}$ plots, Fig. 4(a, b and c), the coefficient $\beta_{exp.}$ can be calculated,. These data are listed also in Table 3. These values are closer to the calculated β_{PF} values at room temperature. Hence, it is suggested that the dominant conduction mechanism is of modified Poole–Frenkle type. The field lowering coefficient $\beta_{exp.}$ increases generally with increasing temperatures and La^{+3} content (see Table 3), which may be due to the free carriers generated thermally [23]. These free carriers act directly to increase the lowering coefficient $\beta_{exp.}$
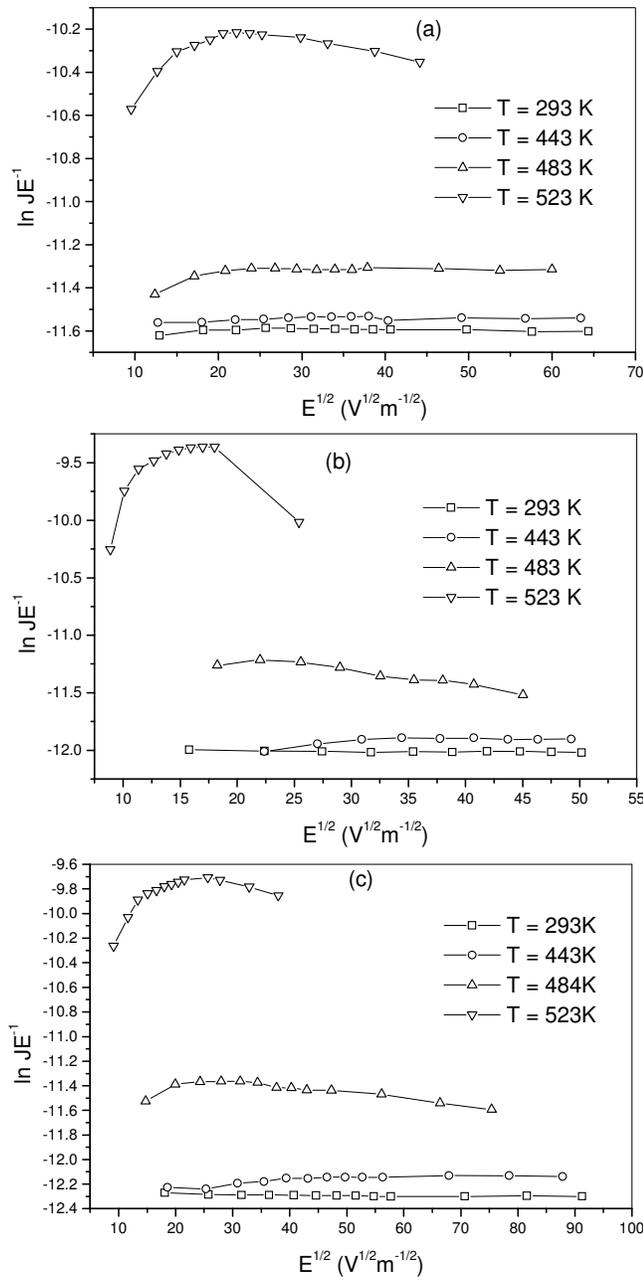
Fig. (4) Plot of ln JE^{-1} versus $E^{1/2}$ for a) $Sr_{0.95}La_{0.05}TiO_3$
b) $Sr_{0.9}La_{0.1}TiO_3$ and c) $Sr_{0.8}La_{0.5}TiO_3$

The effect of composition on the ln J – $E^{1/2}$ characteristics at different temperatures (293 – 523K) can be observed also from Fig. 3 (a, b and c), a decrease in electrical conductivity arises with the increase in the La^{+3} content at room temperature 293K, while the electrical conductivity increases at 523K. It may be due to the charge – compensated by the reduction of a transition metal cation on the B site. Alternatively, the introduction of La^{3+} into a compound $Sr^{+2}TiO_3$ can be accommodated by the introduction of vacancies on the A sublattice [15].

Figure (5) shows the variation of the current density with the reciprocal of the absolute temperature at 10V for different compositions. It is clear that there are two values of the activation energy E_a obtained from this Figure using of the Arrhenius relation:

$$J = J_o \exp (- E_a / k_B T) \tag{3}$$

where k_B is Boltzmanns constant and J_o the pre – exponential factor. The values of activation energy E_a were calculated from the slopes of the curves of Fig. (5) at high temperatures are listed in Table 3. In contrast with the results in [24] the samples considered in the present study show a typical semiconductor-like behaviour with transition temperature $\approx$ 420±5 K, which is agree with others[25]. It was found that the electrical conductivity and E_a decrease with increasing La^{+3} content [8, 25].
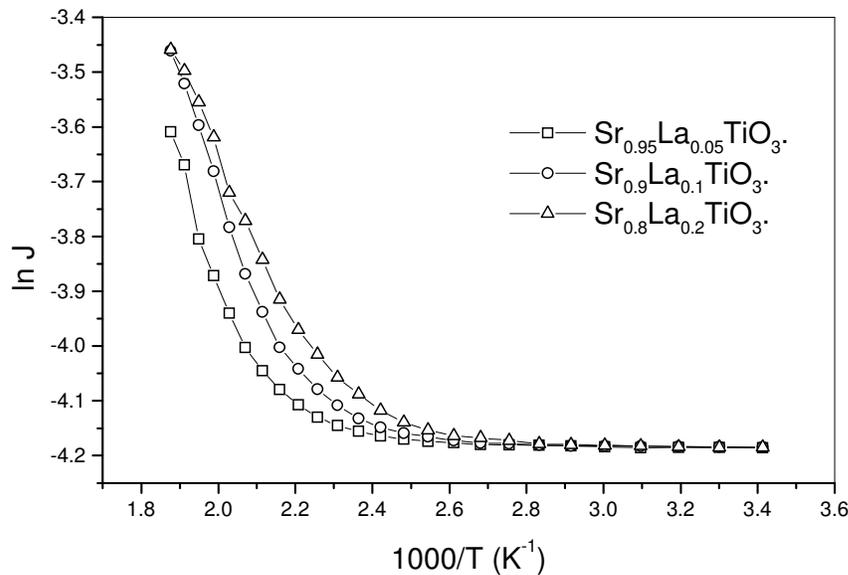
Fig. (5) Plot of ln J versus T^{-1} for SLT ceramics.

4. Conclusion.

X-ray diffraction analysis showed that the investigated compositions are crystalline systems with the perovskite structure in a cubic phase. The conduction mechanisms of perovskite ceramics SLT are analyzed. The modified Poole – Frenkel conduction is the predominant type of conduction in the high voltage region. This was interpreted as due to trapping of charge carriers. The dependence of current on temperature is one corresponding to thermally activated process. The samples possess a typical semiconductor-like behaviour. The increases of La content in the investigated compositions SLT leads to decrease in the electrical conductivity and the activation energy.

References

1. Y.Tokura, Y. Taguchi, Y. Okada, Y. Fujishima, T. Arima, K. Kumagai and Y. Iye, *Phys. Rev. Lett*. **70**, 2126 (1993).
2. K. Kumagai, T. Suzuki, Y. Taguchi, Y. Okada and Y. Fujishima, *Phys. Rev*.; **B 48**, 7636 (1993).
3. P. M. Woodward, *Acta Crystallogr. B* **53**, 44 (1997).
4. J. S. Kim and S. J. L. Kang, *J. Am. Ceram. Soc*. **82**, 119 (1999) and references therein.
5. H. Gränicher and O. Jakits;, *suppl. de nuovo cimento* 11(3), 480 (1954).
6. M. C. McQuarrie, *J. Am. Cer. Soc*. **38** (12), 144 (1955).
7. G. A. Smolenskii, V. A. Isupov, A. I. Agranovskaia and E. D. Sholokhova, *Sov. Phys. Techn. Phys*. **2**, 2351 (1957).
8. H. M. El-Mallah, *Ph.D. Thesis*, Oxford University, U.K (1988).
9. S. A. Howard, J. K. Yau and H. U. Anderson,; *J. Appl. Phys*. **65**, 1492 (1989).
10. M. Eitel and J. E. Greedan, *J. Less-Common Met*. **116**, 95 (1986).
11. T. Mitsui and W. B. Westphan, *Phys. Rev*. **124** (5), 1354 (1961).
12. M. U. Cohen;, *Rev. Sci. Instrum*. **6**, 70 (1935).
13. J. Hutton and R. J. Nelmes, *J. Phys. C: Solid State Phys*. **14**, 1713 (1981).
14. S. A. Howard, J. K. Yau and H. U. Anderson, *J. Appl. Phys*. 65, 1492 (1989).
15. P. D. Battle, J. E. Bennett, J. Sloan, R. J. D. Tilley and J. F. Vente, *J. Solid State Chemistry* **149**, 360 (2000).
16. B. Jaffe, W. R. Cook, H. Jaffe; "*Piezoelectric ceramics*", Academic Press, New York; p. 119 (1971).
17. S. Qin, A. I. Becerro, F. Seifert, J. Gottsmann and J. Jiang, *J. Mater. Chem*. **10**, 1609 (2000).
18. R. D. Shannon, *Acta Crystallogr*. **32**, 751 (1976).
19. A. K. Jonscher, *Thin Films* **1**, 213 (1967).
20. R. M. Hill, *Phil. Mag*. **23**, 59 (1971).
21. T. K. Bansal, S. Bansal and R. G. Mendiratta, *J. Non-Cryst. Solids* **99**, 168 (1988).

22. B. T. Kolomiets, *phys. stat. solidi* **7**, 359 (1964).
23. A. N. Petrov, O. F. Konovchuk, A. V. Andreev, V. A. Cherepanov and P. Kofstad, *Solid State Ionics* **80**, 189 (1995).
24. G. Garcia-Belmonte, J. Bisquert, F. Fabregat, V. Kozhukharov and J. B. Carda, *Solid State Ionics* **107**, 203 (1998).
25. H. M. El-Mallah, *J. Mater. Sci*. **39**, 1 (2004).